Model of Multipath Propagation of Ultrasonic Pulses in Soft Tissue Using Divergent Beam Tomography Method

Jędrzej BOROWSKI, Krzysztof J. OPIELIŃSKI
Faculty of Electronics, Wroclaw University of Science and Technology,
Wybrzeze Wyspianskiego 27, 50-370 Wroclaw, Poland,
jedrzej.borowski@pwr.edu.pl, krzysztof.opielinski@pwr.edu.pl

Abstract

The paper presents the model of calculating ultrasound waveform beam emitted inside the circular space of ultrasonic transducer ring array and propagated through a biological medium submerged in water. Each elementary transducer emits a burst signal, which then propagates through a medium and is received by a number of transducers on the opposite side of the ring array. The method allows for calculating runtime and amplitude of ultrasonic bursts while traveling from an emitter to a receiver through a specified soft tissue section geometry, having regard to the refraction and attenuation effects and directivity pattern of transducers. The soft tissue section geometry is constructed using circular shapes with given ultrasound speed and attenuation distribution. The elaborated software creates a set of received waveforms for each transmitting transducer. The presented results produced by the software can be used as a basis for further research on inverse problems in ultrasound waveform tomography.

Keywords: model of multipath propagation of ultrasonic pulses, ultrasonic transducer ring array, divergent wave beam, soft tissue, ultrasound tomography

1. Introduction

The concept of ultrasound waveform tomography shows much promise as a new method for medical imaging aiding in cancer detection and diagnosis [1, 2]. However, this imaging method is computationally complex, as the inverse problems have to be solved on large amounts of numerical data. We propose a method of generating exemplary data which can be an aid in developing, testing and evaluating algorithms of waveform tomography.

The method is designed to provide exemplary results simulating the behavior of the ultrasound tomography transducer ring array [3, 4], modeled after existing real world implementations. The generated results are simulating the propagation of ultrasonic pulses through biological media submerged in water. The model is highly flexible, allowing for modeling of results for media with various ultrasound speeds and internal composition of the soft tissue section. The elaborated method does not limit the shape of the section. However, the software implementation currently supports the geometry constructed from circular, non-intersecting shapes only. In order to simplify the generation of the results, only refractions and internal reflections of ultrasound beams are taken into consideration.

2. Model of ultrasonic pulse

The ultrasonic pulse is modeled using the equation for linear *burst* type signals [5]:

$$p = p_0 \sum_{n=0}^{\infty} \left(1 - \left| \frac{2t f_0}{m_c} - 1 \right|^m \right) \sin\left(\omega_0 t - \phi_0\right) \tag{1}$$

Where p_0 is the amplitude of acoustic pressure, t is the time, f_0 is the pulse resonant frequency, m_c is the number of sine wave cycles, m is the exponent, which is used to shape the envelope, and $\omega_0 = 2\pi f_0$.

For the purposes of this paper, the generated pulses had the parameters f_0 = 2 MHz, $\varphi_0 = 0$, $m_c = 7$, and the exponent m has the values of $m = 2$ for the first half of the burst, and $m = 0.5$ for the second half. An example of a generated burst is displayed on Fig. 5.

3. Model of transducer directivity

The directivity of each transducer element is modeled to simulate the attenuation of amplitude of the ultrasonic beam which is propagated or received in the transducer at a non-zero angle. The directivity pattern of a rectangular transducer can be calculated from the equation [6]:

$$K(\theta,\varphi) = \left| \frac{\sin\frac{ua}{2}}{\frac{ua}{2}} \right| \left| \frac{\sin\frac{wb}{2}}{\frac{wb}{2}} \right| \tag{2}$$

where $u = (2\pi\sin\theta)/\lambda$, $w = (2\pi\sin\varphi)/\lambda$, a and b are width and height of the transducer, θ is the angle along the OX axis, and φ is the angle along the OY axis. Since the problem is considered in a 2-D environment, it can be assumed that $\varphi = 0$, and the factor containing the w variable can be disregarded:

$$K(\theta) = \left| \frac{\sin\frac{ua}{2}}{\frac{ua}{2}} \right| \tag{3}$$

In the case of narrow rectangular ultrasonic transducers (and so is in this case), better approximation of the directivity pattern gives the formula with the extra $\cos\theta$ factor, which derives from the proper interpretation of the Rayleigh-Sommerfeld theory [7]:

$$g(\theta) = K(\theta) \cdot |\cos\theta| = \left| \frac{\sin\frac{ua}{2}}{\frac{ua}{2}} \cos\theta \right| \tag{4}$$

An example of a directivity pattern generated using the above formula can be seen on Figure 1.

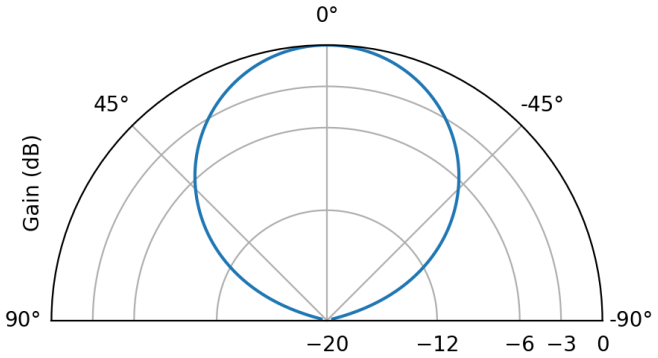

Figure 1. Simulated directivity pattern of a single rectangular transducer in the ring array

4. Model of propagation

The soft tissue geometry is constructed using circular section elements, with given center point (x_0,y_0), radius r, ultrasound speed c, material density ρ, and attenuation distribution a. The transducer ring array is constructed from n^2 emitter-receiver elements and is approximated as a regular circle with the specified radius R. For the purposes of this paper, the geometry of the section placed inside the space of the ring array simulates a breast tissue submerged in water.

The ultrasonic beam is simulated by generating a number of rays from the source origin point, which is located in the middle of the emitting transducer. The rays are generated at angles in the range from -α/2 to α/2, where α is the angular width of the simulated beam. Together with each beam, a simulated pulse waveform is calculated using equation (1). The attenuation and delay of the pulse are applied to the waveform after the propagation is fully simulated. For evaluation, a value of $\alpha = 45°$ was chosen. For adequate simulation accuracy the recommended number of rays is greater or equal to the number of ring array transducers. Additionally, for each ray, the directivity gain g_e of the emitting transducer is calculated using equation (4).

Having computed the directional vectors of each ray, intersections with the nearest soft tissue geometry element can be easily found analytically. For each found point of intersection, the ray is recalculated according to Snell's law. The distance between a previous origin point (e.g. the emitter, or a previous material boundary) is saved together with the information about the ultrasound speed in the medium the ray is currently traversing.

The following equations are used to calculate the ray after colliding with material boundaries, where **I** is the incident ray vector, **N** is the normal vector of the geometry element, **T** is the transmitted ray vector [8], θ_1 and θ_2 are the incidence and refraction angles. The vectors are normalized so that the lengths of both **I** and **T** are equal to 1.

The angle of incidence can be obtained by calculating the dot product of the incident vector and the inverse of the normal vector:

$$\cos\theta_1 = -\mathbf{N}\cdot\mathbf{I} \tag{5}$$

After applying Snell's law, it is possible to calculate the angle of refraction:

$$\sin\theta_2 = \left(\frac{c_2}{c_1}\right)\sin\theta_1 \tag{6}$$

This allows for calculation of the transmitted ray **T** [8]:

$$\mathbf{T} = \frac{c_2}{c_1}\mathbf{I} + \left(\left(\frac{c_2}{c_1}\right)\cos\theta_1 - \sqrt{1-\left(\frac{c_2}{c_1}\right)^2 \sin\theta_1^{\,2}}\right)\mathbf{N} \tag{7}$$

If the calculated angle of refraction is real, then the incident ray is refracted by traversing the element boundary. In this case, it is necessary to calculate the weakness of the ultrasonic pulse. The amplitude transmitting coefficient can be calculated using the following formula [9]:

$$D_p = \frac{\cos\theta_1 - \dfrac{\rho_1 c_1}{\rho_2 c_2}\sqrt{1-\left(\dfrac{c_2}{c_1}\right)^2 \sin^2\theta_1}}{\cos\theta_1 + \dfrac{\rho_1 c_1}{\rho_2 c_2}\sqrt{1-\left(\dfrac{c_2}{c_1}\right)^2 \sin^2\theta_1}} + 1 \tag{8}$$

where θ_1 is the angle of incidence, ρ_1 is the material density of the first environment, ρ_2 is the material density of the second environment, c_1 is the ultrasound speed of the first environment, and c_2 is the ultrasound speed of the second environment.

If the calculated angle of refraction is a complex number, then internal reflection is occurring. In this case, the resulting vector is calculated with the following formula:

$$\mathbf{T} = \mathbf{I} + 2\cos\theta_1\,\mathbf{N} \tag{9}$$

The calculated transmitted vector **T** can be used together with the intersection point to create a new, refracted ray, on which the process can be repeated for the rest of remaining collisions on the path of the ray. When there are no more soft tissue elements for the ray to collide with, an intersection with the transducer ring array is found, and the angle between the propagating ray and the receiving transducer element is calculated. Basing on this angle, the directivity gain for the receiving transducer g_r is calculated using equation (4). Half of the transducers opposite of the emitter are taken into consideration. If the ray collides with a transducer outside of this boundary, it is discarded. The waveform of the propagating ray is added to the input buffer of the receiver transducer.

5. Runtime and amplitude equations

The information gathered allows to calculate the complete waveform of the signal received by the transducer which is hit by the propagated rays. In order to obtain this waveform, the generated pulse must be attenuated and delayed accordingly. The attenuation factor is dependent on the length of the path that the ray has taken through the section geometry, ultrasound speeds of materials passed through, and the number of material boundaries traversed. The equation of the gain can be expressed as:

$$a_p = g_e g_r \prod_{i=1}^{n} s_i a_i \prod_{i=1}^{k} D_i \tag{10}$$

Where g_e is the directivity gain for the emitter transducer, g_r is the directivity gain for the receiver transducer, s_i is the distance and α_i is the attenuation distribution for $i = 1 \ldots n^{\text{th}}$ element passed by the ray, D_i is the transmitting coefficient for $i = 1 \ldots k^{\text{th}}$ material boundary passed by the ray.

The time delay of the received pulse can be expressed as:

$$t_p = \sum_{i=1}^{n} \frac{s_i}{c_i} \tag{11}$$

Where s_i is the distance and c_i is the ultrasound speed of $i = 1 \ldots n^{\text{th}}$ element passed by the ray.

6. Implementation and results

An implementation of this method has been elaborated in Python programming language, using the Shapely library for geometrical computations. The elaborated software is capable of generation and visualization of results of divergent beam tomography. The process can be parametrized by selecting the number of transducers in the ring array, the number of rays simulated in the beam, and the width of the beam. For each emitting transducer, the software generates a set of waveforms received by the receiving transducers.

Figure 2 presents examples of the modelling of the paths taken by the rays in the ultrasound beam. In this example, a beam of 32 rays with the width of 45° has been propagated through a medium submerged in water. In the left example, the element has a higher ultrasound speed than that in the water, and in the right example, the ultrasound speed in the element is lower than that in the water. It can be seen how the introduction of the tissue into the water is affecting the ultrasound beam.

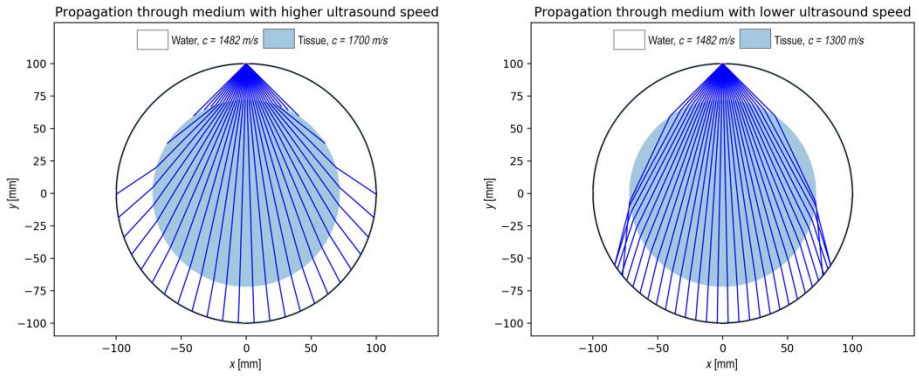

Figure 2. Examples of the modeled ray paths in the ultrasound beams passing through higher and lower sound speed media

Figure 3 presents a modeled propagation through a complex medium - a soft tissue section which contains elements with three different ultrasound speed values. The ultrasound speed of the main element is similar to the sound speed of tissue such as a female breast. The other ultrasound speed values have been chosen to visualize the focusing and scattering of the beams. The right side of the figure presents a selection of received waveforms from the aforementioned example. It can be seen how the angle of the beam, distance traveled by the ultrasound pulse, and the presence of tissue on its way affects the amplitude and time delay of the signal. The received waveforms are numbered from 1 to 25, and the locations of the transducers that received those waveforms are marked on the left plot. A number of the received waveforms, e.g. numbered 10, 18, and 21 are a result of multiple beams entering the same receiver transducer. In this case, it can be observed that the waveforms of the received signals are amplified or attenuated due to summing of signals incoming to the receiver.

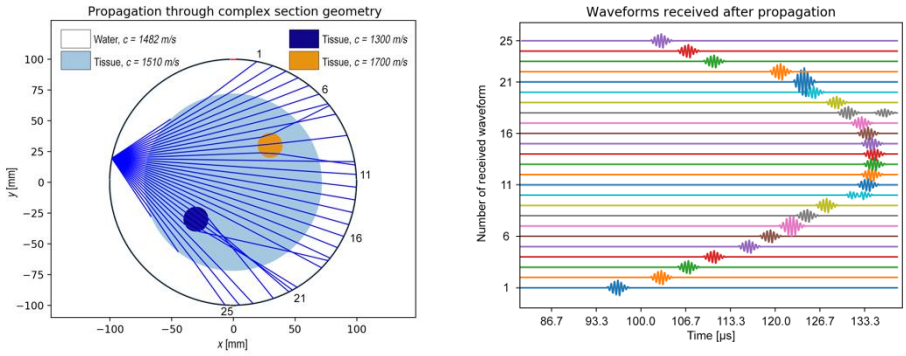

Figure 3. Example of the modeled ray paths in a complex section geometry, and a selection of waveforms received by the simulated transducer

Figure 4 shows another example of propagation through the complex geometry, where the differences between sound speeds of the elements are smaller than in the previous example. Focusing of the beams on the elements with lower sound speed (beams 18 to 20) and scattering of the beams on elements with higher sound speed (beams 9 to 11) can be observed. Beams 13 to 16 are passing through an object with lower sound speed first, and an object with higher sound speed second. This example presents that the model is capable of calculating many refractions for each beam.

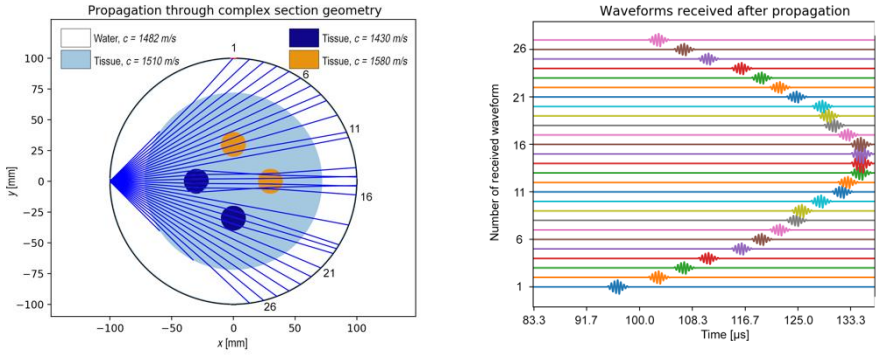

Figure 4. Example of propagation through a section with elements of varying sound speed, and the waveforms received by the simulated transducer

Figure 5 presents an example of an ultrasound pulse waveform before and after propagating through a complex section geometry. This example was generated using 1024 transducer elements, and 1024 rays for each propagation. Due to multipath nature of the elaborated method, the receiving transducer has been hit by many rays at different times, causing changes in the envelope of the received signal.

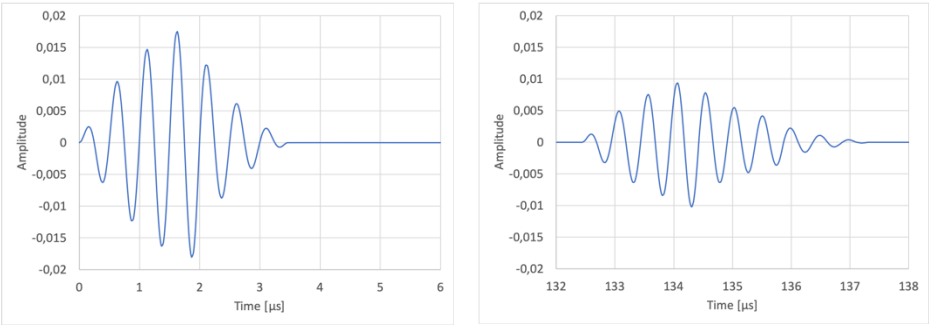

Figure 5. Examples of the generated pulse waveform before and after propagating through a system

7. Conclusions

The elaborated method allows for effective, and computationally inexpensive generation of exemplary results of ultrasound tomographic measurements, which can be used as reference measurements in the development of ultrasound waveform tomography algorithms. The flexible geometry and possibility of parametrizing results allows for analysis of factors such as the number of transducers, their directivity, and the size of the ring array on measurement results. The elaborated software due implementation can also be useful as a teaching aid to explain basic ultrasonic wave propagation phenomena using the implemented visualization methods.

References

1. G. Sandhu, C. Li, O. Roy, S. Schmidt, N. Duric, *High-resolution quantitative whole-breast ultrasound: in vivo application using frequency-domain waveform tomography*, in [SPIE Medical Imaging], 94190D-94190D, International Society for Optics and Photonics (2015).
2. G. Sandhu, C. Li, O. Roy, E. West, K. Montgomery, M. Boone, N. Duric, *Frequency-domain ultrasound waveform tomography breast attenuation imaging*, in [SPIE Medical Imaging], 97900C-97900C, International Society for Optics and Photonics (2016).
3. T. Gudra, K. J. Opieliński, *The ultrasonic probe for the investigating of internal object structure by ultrasound transmission tomography*, Ultrasonics, **44**(1-4) (2006) e295 – e302.
4. K. J. Opieliński, P. Pruchnicki, P. Szymanowski, W. K. Szepieniec, H. Szweda, E. Świś, M. Jóźwik, M. Tenderenda, M. Bułkowski, *Multimodal ultrasound computer-assisted tomography: An approach to the recognition of breast lesions*, Computerized Medical Imaging and Graphics, **65** (2018) 102 – 114.
5. K. Opieliński, *Analysis and modelling of ultrasonic pulses in a biological medium*, Archives of Acoustics, **33**(4) (2008) 13 – 19.
6. H. F. Olson, *Acoustical Engineering*, D. Van Nostrand Company, New Jersey 1957.
7. A. R. Selfridge, G. S. Kino, B. T. Khuri-Yakub, *A theory for the radiation pattern of a narrow-strip acoustic transducer*, Appl. Phys. Lett., **37**(1) (1980) 35 – 36.
8. A. S. Glassner, *An Introduction to Ray Tracing*, Academic Press, Palo Alto 1989.
9. J. Obraz, *Ultrazvuk v měřicí technice*, SNTL, Praha 1984.